Analysis of multiplier with a novel symmetric ferroelectric varactor

Pär Rundqvist*, Andrei Vorobiev*, Spartak Gevorgian* † and Erik Kollberg*
*Department of Microtechnology and Nanoscience
Chalmers University of Technology
SE-412 96 Göteborg, Sweden
Email: par.rundqvist@mc2.chalmers.se
†Microwave and High Speed Electronics Research Center
Ericsson AB,
SE-431 84 Mölndal Sweden

***Abstract*— This work is aimed at investigating the potential of $(\mathbf{Ba}, \mathbf{Sr})\mathbf{TiO_3}$ ferroelectric varactors in frequency multipliers in the 100 GHz to several THz region. There has been an increasing interest frequency generation in this frequency band in recent years. An equivalent circuit is introduced with a voltage dependent capacitance $\mathbf{C}(\mathbf{V})$, constant resistances and constant inductance components, to describe the impedance and multiplier behavior over a wide frequency range. The measured C-V curve is similar to that of the Heterostructure Barrier Varactors (HBV). The components values are extracted using a random optimisation method. As the thin film measurements are limited to frequencies below 50 GHz, the equivalent circuit parameters are also fitted using measured bulk data. The cut-off frequency is approximately 3 THz, which is slightly higher than initially obtained with HBVs. Harmonic balance simulations show an efficiency of around 5% for a 3x300 GHz multiplier. Our results show that the ferroelectric varactor has an interesting potential for applications in frequency multipliers at submillimetre waves and THz frequencies.**

I. Introduction

In recent years there has been an increasing interest of power generation in the lower THz region [1]. The main applications are within science, spectroscopy, radio astronomy and future communication technologies. However at frequencies of one to a few THz, there is a drop in output power of the currently available sources. This region is known as the THz gap.

Several techniques are under investigation to fill this gap, including varactor multipliers. The varactor multipliers can be divided into two categories depending on the appearance of the C-V curve, symmetric or asymmetric. A typical example of the asymmetric C-V curves is displayed by Schottky diodes. A Schottky diode in a multiplier will therefore generate both even and odd harmonics. The Heterostructure Barrier Varactor (HBV) on the other hand displays a symmetric C-V curve. The absence of even harmonics in a symmetric varactor multipliers simplifies the realisation of higher order multiplier circuits. The potential of HBV varactors has already been proven in real circuits [2].

For multiplier applications the limiting properties of varactor are the breakdown voltage, resistive losses, and the tunability of the capacitance (magnitude and shape) [3]. Ferroelectric varactors using $(\mathrm{Ba}, \mathrm{Sr})\mathrm{TiO_3}$ (BST) have high breakdown voltage, very low resistive losses, considerable tuning, high speed and are easily scalable [4], [5], [6]. Apart from this, BST varactors are integratable on Si and have a rather simple structure compared to the HBV [7]. It should be pointed out that in ferroelectric materials the change in capacitance is due to field dependent polarisation. In semiconductor devices the capacitance changes due to electrons moving causing a depleted region. There is a certain inertia in electrons that are not present when moving polarisations. All of this makes the ferroelectric varactor a promising candidate for multipliers in the THz gap.

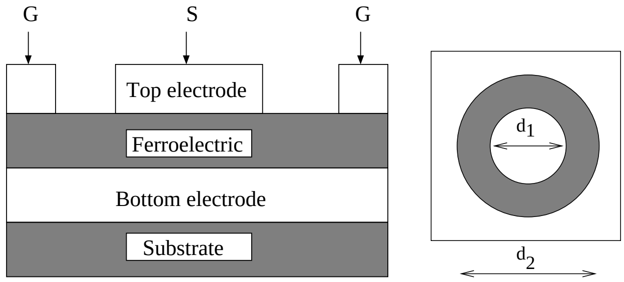

(a) Cross section (b) Layout

Fig. 1. Cross section (a) and layout (b) of the varactor.

In this paper we investigate the potential of a ferroelectric varactor made from $(\mathrm{Ba}, \mathrm{Sr})\mathrm{TiO_3}$ in a frequency multiplier using harmonic balance simulations.

II. Experimental

High resistivity ($\rho_{Si} = 5\mathrm{k}\Omega \cdot \mathrm{cm}$) platinized silicon $\mathrm{Pt}/\mathrm{TiO_2}/\mathrm{SiO_2}/\mathrm{Si}(100)$ was used as substrate. Pt (50 nm)/Au (500 nm) bottom electrode films were deposited by e-beam evaporation at room temperature. 300 nm BST was deposited by pulsed laser ablation from a $\mathrm{Ba_{0.25}Sr_{0.75}TiO_x}$ target at $650°$ C and 0.4 mBar oxygen pressure using a KrF examiner laser (λ = 248 nm, τ =30 ns) operating at 10 Hz with an energy density of 1.5 $\mathrm{J} \cdot \mathrm{cm}^{-2}$. After deposition, the sample was cooled down to room temperature at 950 mBar oxygen pressure. The Au (500 nm)/Pt (50 nm) top electrode films were

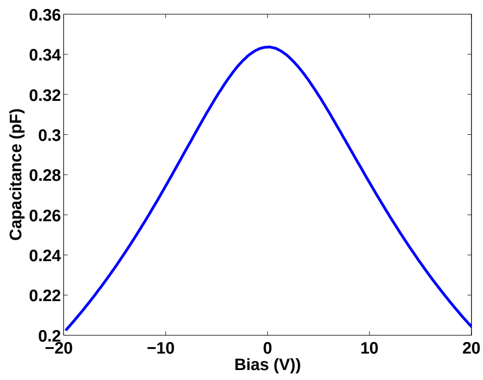

Fig. 2. Capacitance vs. DC bias at 1 MHz.

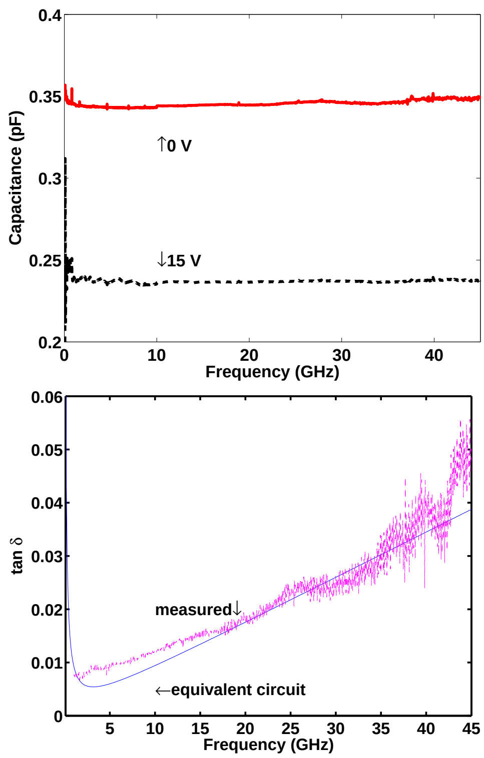

Fig. 3. The capacitance at 0V and 15v dc bias (a) vs. frequency. Measured and calculated (from the equivalent circuit) $\tan\delta$ (b) vs. frequency.

also deposited by e-beam evaporation at room temperature, Fig. 1(a). The top electrodes were patterned with a lift-off process. The layout of the top electrode consists of a central circular patch (d_1 =10 μm or d_1 =30 μm in diameter) and a co-centric outer electrode with d_2 =150 μm internal diameter as seen in Fig. 1(b). The size of the outer electrode can be considered infinite (5x5 mm).

The C-V characteristic was measured at 1 MHz using an HP LCR meter on a $d_1 = 30$ μm electrode. S_{11} was measured using a Vector Network Analyser between 45 MHz and 45 GHz connected to a top electrode with $d_1 = 10$ μm in diameter. The size of the outer electrode is for both structures d_2 =150 μm. The capacitance, tunability and $\tan\delta$ were extracted from the S_{11} measurement using methods presented in a previous work [8].

III. The Equivalent Circuit

The C-V curve shown in Fig. 2 is measured at 1 MHz. Note that the capacitance is measured using the larger (d_1 =30 μm) top electrode. The capacitance is easily rescaled to a (d_1 =10 μm) top electrode, in order to be easy comparable to the high frequency measurements, using Eq. 1. The capacitance of a parallel plate varactor is calculated as:

$$C = \frac{\epsilon_0 \epsilon S}{t} \tag{1}$$

where S is the surface area of the top electrode; t is the thickness of the ferroelectric film; $\epsilon_0 = 8.85 \cdot 10^{-12}$ (F/m) is the dielectric constant of the vacuum and ϵ ($\epsilon_{max} \approx 200$) is the permittivity of the ferroelectric film. The rescaled capacitance is used in further simulations.

Fig. 3(a) shows the capacitance of the varactor at 0 V and at 15 V DC-bias. It can be seen that the permittivity is frequency independent between 100 MHz and 45 GHz both at 0 V and 15 V. By comparing Fig. 3(a) and Fig. 2 we see that the maximum and minimum of capacitance is preserved. The tunability is calculated as:

$$T = \frac{C(V_{Max}) - C(V_{Min})}{C(V_{Max})} = \frac{C(E_{Max}) - C(E_{Min})}{C(E_{Max})} \approx 41\% \tag{2}$$

which is also frequency independent. We can anticipate a larger tunability with more applied DC bias. As these measurements are limited in frequency, due to the measurement set up, we have to rely upon STO bulk data [9], [10] for an extrapolation to higher frequencies. The bulk permittivity is essentially frequency independent up to 3 THz.

In Fig. 3(b) $\tan\delta$ can be seen as a function of frequency. $\tan\delta$ for the Device Under Test (DUT) is 0.04 at 45 GHz. However from [8] we can calculate that $\tan\delta$ in the film is 0.015 at 45 GHz. The intrinsic losses for bulk BST is 0.002 at 10 GHz and room temperature [10]. This means that the extrinsic losses are about 5 times higher than the intrinsic losses at 10 GHz. The origin of the fundamental (intrinsic) loss is the interaction of the ac-field with the phonons of the material. The extrinsic losses are associated with coupling of the ac-field with defects. Among the known extrinsic loss mechanisms those listed below are considered as significantly contributing to the loss in the tunable microwave materials [6], [11]:

1) Loss owing to charged defects.
2) Universal relaxation low mechanism.
3) Quasi-Debye contribution induced by random-field defects.

The pure intrinsic losses are increasing as f^1 [6] and the extrinsic losses, due to charged defects, increases as $f^{1/3}$ [11], [13]. The losses in the electrode increases as $f^{1/2}$ [11]. The extrinsic losses are dominating at lower frequencies and the intrinsic at higher .

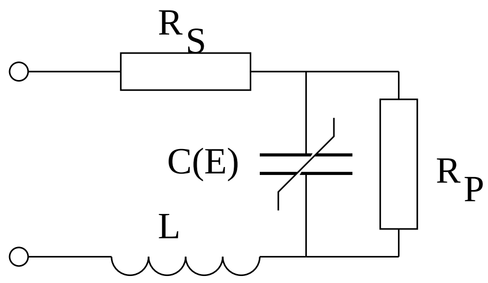

Fig. 4. Simplified equivalent circuits of the varactor.

With the measured and extracted results we now can determine an equivalent circuit. The capacitance is already found in Fig. 3(a). Looking at the physical structure in Fig. 1(a) and 1(b) we arrive at a rather complex equivalent circuit, which can be simplified [8]. The simplified circuit is shown in Fig. 4. The reason for an inductance in the equivalent circuit is to model the increase in $\tan\delta$ appearing in STO up to 3 THz [9]. The parameter values are found using a random optimisation method and comparing both thinfilm and bulk data. The voltage independent values are $L = 8.3$ fH, $R_S = 0.11\ \Omega$, $R_P = 3000\ \Omega$ and the capacitance varies in between $C_{Min} = 0.20$ and $C_{Max} = 0.34$ pF. From these parameters $\tan\delta$ can be calculated:

$$\tan\delta = \frac{Re(Z)}{Im(Z)} \tag{3}$$

the result is plotted as equivalent circuit in Fig. 3(b). Now that all the parameters in the equivalent circuit are determined we can calculate the cut-off frequency useful for comparison to other varactors.

$$f_c = \frac{1/C_{Min} - 1/C_{Max}}{2\pi R_S} \tag{4}$$

In the above equation the inductance and parallel resistance are neglected. We can now see that the cut-off frequency is 3 THz, which is the same order as for HBVs [2], [3]. The limit of 20 V in voltage swing is mainly due to the measurement set-up. We estimate by using a higher applied voltage we would reach $C_{Min} = 0.17$ pF. This would increase the cut off frequency 40 %. Even if the cut-off frequency is an important figure-of-merit regarding a varactor in a multiplier, it does not say everything. As already stated the shape of the C-V curve has a substantial influence on the varactor performance [3]. The C-V dependence in Fig. 2 can be considered as symmetric and can be therefore be described as [12]:

$$C(E) = 3.4 \cdot 10^{-13} + 1.5 \cdot 10^{-3} E^2 \tag{5}$$

Equation (5) is expressed in the electric field E(V/m) instead of applied bias voltage because of the scalability of ferroelectric varactors. If the fringing fields are ignored then the top electrode can be made as small as manufacturing tolerances (1 nm). However the fringing field must be included when the radius of the top electrode becomes comparable to the thickness [12]. The minimum thickness of the ferroelectric film is limited by the dead-layer effect [7], [11]. The dead-layer is caused by an approximately 20 nm thick layer in the ferroelectric, close to a metal electrode. This sets the lowest limits of the film thickness. The nature of dead layers are not completely understood but is usually associated with interdiffusion, chemical reactions, contamination and/or structural defects in the metal/ferroelectrics interfaces [13]. The problem is most pronounced in the ferroelectric film close to the bottom electrode. The influence of the dead layer can be reduced by using a $SrRuO_3$ (SRO) interlayer [11]. A SRO interlayer will increase $\tan\delta$. However also the capacitance (two times) and tunability (> 60 %) will increase. The cut-off frequency, however, will be approximately the same as without SRO interlayer [14].

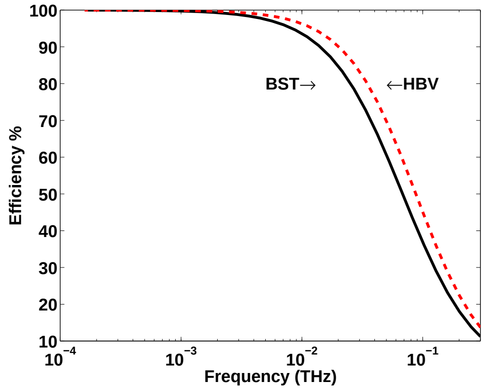

Fig. 5. The conversion efficiency for the tripler as a function of the pump frequency f_p

IV. Tripler performance

An in-house harmonic balance (HB) simulator was used to calculate the conversion efficiency for the third order harmonics. We used 15 dBm input power, the C-V dependence in Eq. (5), (Fig. 2) and the equivalent circuit shown in Fig. 4 in the simulations. The resulting efficiency is shown in Fig. 5. Also shown is a curve for the empirical expression for HBV tripler:

$$\eta = \frac{100}{1 + \alpha(\frac{n \cdot f_p}{3 \cdot f_c})^{\beta}} \tag{6}$$

Where $\alpha = 200$ and $\beta = 1.5$ are empirically determined and n is the order of the multiplication [15]. These results are confirmed for higher frequencies by a commercially available ADS HB simulator. The efficiency for the ferroelectric varactor is close to 100% for lower frequencies with a rapid decrease as the frequencies approaches the cut-off frequency. This is in correspondence with results presented on HBVs [3]. Compared to these HBVs the series resistance R_S is lower but the tunability is also lower. One major contributor to the lower tunability is material defects in the ferroelectric thin film, strains and film interfaces to metal electrodes.

V. Accuracy

When making HB simulations, the accuracy of the parameters involved is very important. In a previous paper we reported that the error in both C and $\tan\delta$ is less than $\pm 10\%$ [8]. As R_S is derived from the S_{11} measurement in the same manner as C, the error can be estimated to be less than $\pm 15\%$. The HB simulations are very sensitive to error in R_S [3]. If we start by considering the possible error in the cut-off frequency Eq. (1), we have:

$$\Delta f_c < |f_c \frac{\Delta R_S}{R_S}| + 2|f_c \frac{\Delta C}{C_{Min}}| \approx 0.35 f_c \qquad (7)$$

This shows that the error in cut-off frequency can be as large as 35% or 1 THz. As we have seen before the efficiency is very dependent on the cut-off frequency and thereby R_S and C. Dillner et al have investigated the large influence in the efficiency of any change in R_S. [3].

VI. Discussion and conclusion

This work is aimed at investigating the potential of $(\mathrm{Ba,Sr})\mathrm{TiO_3}$ ferroelectric devices for THz multiplier applications. A simple equivalent circuit is used to achieve foundations for harmonic balance simulations. The equivalent circuit ($L = 1.5$ fH, $R_S = 0.11\Omega$, $R_P = 3000\Omega$, $C_{Min} = 0.20$ and $C_{Max} = 0.34$ pF) is designed to describe the frequency dependence of both $\tan\delta$ and the impedance of the device. The cut-off frequency of the device is approximately 3 THz, which is of the same order of magnitude as the HBVs. Harmonic balance simulations show an efficiency of around 5 % for a 3x300 GHz multiplier. All this put together shows that the ferroelectric varactor has potential for frequency multipliers in the THz region. However the results are very dependent on material properties, the losses increased and the tunability decreased for thin films compared to bulk. At the same time the integration of a simple technology on Si is vital for future applications.

Our results show that the ferroelectric varactor has an interesting potential for applications in frequency multipliers at submillimetre waves and THz frequencies.

Acknowledgment

This work was supported by Swedish Strategic Research Foundation SSF (Oxide and HSEP Research center), VR project components for future microwave systems, Ericsson AB and Vinnova (PIDEA/Pacific boat). Thank you Bahar M. Motlagh and Sten Gunnarsson for the help with ADS and Jan Stake for help with the in-house HB simulator.

References

[1] P. H. Siegel, *"Terahertz technology in biology and medicine"* IEEE trans Microwave Theory and Techn. 52, no 10 2438 (2004).

[2] M. Ingvarsson, A. Ø. Olsen, J. Stake, *"Design and analysis of 500 GHz heterostructure barrier varactor quintuplers"* Proc. 14th international symposium on space terahertz tech. 2003.

[3] L. Dillner, J. Stake, E. L. Kollberg *"Analysis of symmetric varacrtor frequency multipliers"* Microwave Opt. Techn. Lett. Vol 15.

[4] S. Gevorgian, E. Kollberg, *"Do we really need ferroelectrics in paraelectric state only in electrically controlled microwave devices?"* Asia-Pacific Microwave Conference Proceedings, APMC, 2000, p 23

[5] A. Vorobiev, P. Rundqvist, K. Khamchane, S. Gevorgian, *"Silicon substrate integrated high Q-factor parallel-plate ferroelectric varactors for microwave/millimeterwave applications"* Appl Phys Lett 83, 3144 (2003).

[6] A. K. Tagantsev, V. O. Sherman, K. F. Astafiev, J. Venkatesh, N. Setter *"Ferroelectric materials for microwave tunable applications"* J. Electr. Cer. Vol 11, pp. 5-66 (2003).

[7] R. York, A. Nagra, E. Erker, T. Taylor, P. Periaswamy, J. Speck, S. Streiffer, O. Auciello, *"Microwave integrated circuits using thin-film BST"* IEEE International Symposium on Applications of Ferroelectrics, v 1, 2000, p 195-200.

[8] P. Rundqvist, A. Vorobiev, S. Gevorgian, *"Non-destructive microwave characterisation of ferroelectric films on conductive substrates"* Intrg. Ferroelectr. 60:1-19, 2004.

[9] J. Petzelt, T. Ostapchuk, I. Gregora, I. Rychetsky, S. Hoffmann-Eifert, A. V. Pronin, Y. Yuzyuk, B. P. Gorshunov, S. Kamba, V. Bovtun, J. Pokorny, M. Savinov, V. Porokhonskyy, D. Rafaja, P. Vanek, A. Almeida, M. R. Chaves, A. A. Volkov, M. Dressel, R. Waser, *"Dielectric, infrared, and Raman response of undoped $SrTiO_3$ ceramics: Evidence of polar grain boundaries"* Phys. Rev. B (Condensed Matter and Materials Physics), v 64, n 18, 1 Nov. 2001, p 184111/1-10.

[10] K. Bethe, Philips Res. Repts. Suppl. 2, 74, Eindhoven, Netherlands: N. V. Philips' Gloeilampenfabrieken, 1970, pp. 55-97.

[11] A. Vorobiev P. Rundqvist S. Gevorgian, *"Microwave loss mechanism in $Ba_{0.25}Sr_{0.75}TiO_3$ thin film varactors"* J. Appl. Phys.

[12] J. Im, S. K. Streiffer, O. Auciello, A. R. Krauss, *"$Ba_xSr_{1-x}Ti_{1+y}O_{3+z}$ interface contamination and its effect on electrical properties"* Applied Physics Letters, v 77, n 16, 16 Oct. 2000, p 2593-5

[13] P. Rundqvist, A. Vorobiev, S. Gevorgian, *"Large Signal Circuit Model of Parallel-Plate Ferroelectric Varactors"* European Microwave Conference, Amsterdam Nederlands, EuMC Oct, 2004.

[14] P. Rundqvist, A. Vorobiev, S. Gevorgian, *"Influence of $SrRuO_3$ interlayer in ferroelectric BST varactors"* To be published.

[15] J. Stake, S. H. Jones, L. Dillner, S. Hollung, E. L. Kollberg, *"Heterostructure-barrier-varactor design"* IEEE Trans. on Microwave Theory Tech, vol. 48, pp 677 - 682, 2000